

Collagen peptides from soft-shelled turtle induce calpain-1 expression and regulate inflammatory cytokine expression in HaCaT human skin keratinocytes

TETSUSHI YAMAMOTO, SAORI NAKANISHI, KUNIKO MITAMURA and ATSUSHI TAGA

Pathological and Biomolecule Analyses Laboratory, Faculty of Pharmacy,
Kindai University, Higashi-Osaka, Osaka 577-8502, Japan

Received December 26, 2017; Accepted May 3, 2018

DOI: 10.3892/ijmm.2018.3659

Abstract. Collagen peptides (CPs), derived by hydrolyzing collagen with chemicals or enzymes, are often used as functional materials, due to their various bioactivities and high bioavailability. A previous study by our group reported that collagen from soft-shelled turtle, *Pelodiscus sinensis*, induces keratinocytes to undergo epithelial-mesenchymal transition and facilitates wound healing. Therefore, CPs derived from soft-shelled turtle collagen may have useful effects on the skin. In the present study, the functional effects of CPs on human skin were examined by analyzing CP-treated human keratinocytes with a shotgun liquid chromatography/mass spectrometry-based global proteomic approach. A semi-quantitative method based on spectral counting was applied and 211 proteins that exhibited >2-fold changes in expression after CP treatment were successfully identified. Based on a Gene Ontology analysis, the functions of these proteins were indicated to be closely linked with protein processing. In addition, CP treatment significantly increased the expression of calpain-1, a calcium-dependent intracellular cysteine protease. Furthermore, CP-treated keratinocytes exhibited elevated interleukin (IL)-1 α and IL-8 expression and reduced IL-6 expression. CPs also induced the expression of proteins implicated in cell-cell adhesion and the skin barrier. Therefore, CPs from soft-shelled turtle may provide significant

benefits for maintaining the biological environment of the skin, and may be useful as components of pharmaceuticals and medical products.

Introduction

Collagen is a ubiquitous structural protein. There are more than 20 different types of collagen, with specific functions in each tissue (1,2). These proteins have important roles in the maintenance of the extracellular matrix environment (3-7). Certain studies have demonstrated that collagen regulates cell proliferation or apoptosis (8,9). In this decade, collagens of marine origin (e.g., fish, sponges and mollusks) have been considered a useful resource due to their high availability (10-17). These collagens have been widely used as functional foods or dietary supplements. Collagen has also been used for skin substitutes and drug delivery vehicles (18-23).

Recently, collagen peptides (CPs), derived from chemical and enzymatic collagen hydrolysis (24,25), have been increasingly used as functional materials, due to their various bioactivities and high bioavailability (26,27). Several studies have demonstrated the beneficial effects of CPs. For instance, CPs derived from fish skin were demonstrated to have several protective effects on skin photo-aging and wound healing, as they improved moisture retention and repaired endogenous collagen and elastin protein fibers (28-32). Therefore, CPs are considered a useful material for the development of cosmetics, pharmaceuticals and medical products.

Previous studies by our group reported that tissue from soft-shelled turtle, *Pelodiscus sinensis*, may be a useful alternative source of collagen (33). Due its ability to induce keratinocytes to enter the epithelial-mesenchymal transition (EMT), which facilitates wound healing, this collagen may be a useful component of pharmaceuticals and medical products (34). Furthermore, CPs from soft-shelled turtle may have beneficial effects on skin. However, due to differences in habitat environments, collagen from soft-shelled turtle may differ greatly from collagen from mammalian or marine sources, in terms of physicochemical properties, amino acid composition and physiological functions. Therefore, further research is required prior to the use of CPs derived from soft-shelled turtle tissue in commercial products.

Correspondence to: Dr Atsushi Taga, Pathological and Biomolecule Analyses Laboratory, Faculty of Pharmacy, Kindai University, 3-4-1 Kowakae, Higashi-Osaka, Osaka 577-8502, Japan
E-mail: punk@phar.kindai.ac.jp

Abbreviations: MALDI-TOF/MS, matrix-assisted laser desorption-time of flight/mass spectrometry; LC-MS/MS, liquid chromatography tandem mass spectrometry; NSAF, normalized spectral abundance factor; RT-PCR, reverse transcription-polymerase chain reaction; IL, interleukin; TNF, tumor necrosis factor

Key words: collagen peptide, proteomics, soft-shelled turtle, calpain-1, cytokine

In the present study, a shotgun liquid chromatography/mass spectrometry (LC/MS)-based global proteomic analysis of human keratinocytes treated with CPs was performed to examine the functional effects of CPs on human skin. A total of 211 differentially expressed proteins was identified in keratinocytes treated with CPs compared with untreated keratinocytes. It was investigated whether any of these proteins may be involved in the induction of inflammatory factors in human skin.

Materials and methods

Chemicals and reagents. The highest-grade chemicals and reagents available were purchased from Wako Pure Chemical Industries (Osaka, Japan). Emperor tissue, a soft tissue in the region around the shell of soft-shelled turtles (*P. sinensis*), was provided by Shin-uoei, Inc. (Osaka, Japan).

Collagen extraction. Collagen extraction was performed as described in a previous study (33). In brief, emperor tissue was treated with 0.1 M formic acid at a ratio of 1:10 (w/v) for 24 h for demineralization. The sample was then treated with 0.1 M NaOH at a ratio of 1:10 (w/v) for 3 days to remove non-collagenous proteins, including endogenous proteases. The NaOH solution was changed every day. Finally, the sample was incubated with 0.03 M citric acid for 24 h. After the incubation, the solution was centrifuged at $6,500 \times g$ for 20 min at 4°C, and the supernatant was collected. This collagen solution was used in the subsequent experiments.

Tryptic digestion of collagen. The extracted collagen solution was subjected to proteolytic activation with bovine pancreatic trypsin (Sigma-Aldrich; Merck KGaA, Darmstadt, Germany) in 100 mM ammonium bicarbonate buffer (pH 8.0). The collagen was incubated with trypsin at a trypsin/collagen ratio of 1:100 (w:w) at 37°C. At each indicated time-point, reaction solutions were quickly removed and heated to 100°C to terminate trypsin digestion.

Tricine-SDS-PAGE. The molecular weights of the tryptic digestion products were determined with tricine-SDS-PAGE, as described previously (35). For comparison, molecular weight markers ranging from 3.5 to 42 kDa (Wako Pure Chemical Industries) were used. The electrophoresed gel was stained with Coomassie brilliant blue at room temperature for 1 h.

Matrix-assisted laser desorption-time of flight/mass spectrometry (MALDI-TOF/MS). CPs were applied onto the MALDI target plate (Shimadzu, Kyoto, Japan) with 10 mg/ml of α -cyano-4-hydroxy cinnamic acid (Sigma-Aldrich; Merck KGaA) in 50% acetonitrile and 0.05% trifluoroacetic acid. The mass spectra of the CPs were determined with an AXIMA Confidence (Shimadzu) in reflector mode. Prior to acquiring the peptide mass spectrum of the sample, the system was calibrated with a ProteoMass Peptide & Protein MALDI-MS Calibration Kit (cat. no. MSCAL1-1KT; Bradykinin fragment 1-7, 757.3997; P₁₄R, 1,533.8582; insulin oxidized B-chain, 3,494.6513; Sigma-Aldrich; Merck KGaA).

Cell culture. HaCaT immortalized human keratinocytes were purchased from CLS Cell Lines Service GmbH (Eppenheim,

Germany). The cells were cultured in RPMI-1640 medium supplemented with 10% fetal bovine serum (Gibco; Thermo Fisher Scientific, Inc., Waltham, MA, USA) in an atmosphere containing 5% CO₂ at 37°C.

Cell growth assay. Cells were plated at a density of 5×10^3 cells/well in a 96-well plate and grown in culture medium. The medium was changed the next day, and different concentrations of CPs were added. After 72-h treatments, the cells were incubated with the WST-8 cell counting reagent (Wako Pure Chemical Industries), and the optical density of the culture solution was measured at 450 nm with an ELISA plate reader.

Protein preparation. HaCaT cells were plated in a 60-mm dish at a density of 2×10^5 cells per dish and grown in culture medium. The medium was changed the next day and CPs were added. After 72-h treatments, the cells were solubilized in urea lysis buffer (7 M urea, 2 M thiourea, 5% CHAPS, 1% Triton X-100). The protein concentration was measured with the Bio-Rad Protein Assay (cat. no. 5000006JA; Bio-Rad Laboratories, Hercules, CA, USA).

In-solution trypsin digestion. The gel-free digestion method was applied as described previously (36). In brief, 10 μ g protein extract from each sample was chemically reduced by adding 45 mM dithiothreitol and 20 mM tris(2-carboxyethyl)phosphine. Subsequently, the protein was alkylated with 100 mM iodoacetamide. After the alkylation, the samples were digested with mass spectrometry grade trypsin gold (Promega Corp., Madison, WI, USA) at 37°C for 24 h. Next, the digests were purified with PepClean C-18 Spin Columns (Thermo Fisher Scientific, Inc.) according to the manufacturer's protocol.

Liquid chromatography tandem MS (LC-MS/MS) analysis for protein identification. Peptide samples ($\sim 2 \mu$ g) were injected into a peptide L-trap column (Chemicals Evaluation and Research Institute, Tokyo, Japan) with an HTC PAL autosampler (CTC Analytics, Zwingen, Switzerland). The peptides were separated further in a Paradigm MS4 (AMR Inc., Tokyo, Japan) with a reverse-phase C18-column (L-column, 3- μ m-diameter gel particles and 120 Å pore size, 0.2x150 mm, Chemicals Evaluation and Research Institute). The mobile phase consisted of 0.1% formic acid in water (solution A) and acetonitrile (solution B). The column flow rate was 1 μ l/min with a concentration gradient of 5% B to 40% B over 120 min. Gradient-eluted peptides were analyzed with an LTQ ion-trap mass spectrometer (Thermo Fisher Scientific, Inc.). The results were acquired in a data-dependent manner, where MS/MS fragmentation was performed on the two most intense peaks of each full MS scan.

All MS/MS spectral data were entered into a search for comparisons against the SwissProt *Homo sapiens* database with the Mascot tool (version 2.4.01; Matrix Science, London, UK). The search criteria were as follows: Enzyme, trypsin; with the following allowances: Up to two missed cleavage peptides; mass tolerance, ± 2.0 kDa; MS/MS tolerance, ± 0.8 kDa; and cysteine carbamidomethylation and methionine oxidation modifications.

Semiquantitative analysis of identified proteins. The fold-change in expression was calculated as the log₂ of the

ratio of protein abundances (Rsc), evaluated by spectral counting (37). For comparison, the relative amounts of identified proteins were calculated using the normalized spectral abundance factor (NSAF) (38). Differential expression of proteins were considered significant when the Rsc was >1 or <-1 , which corresponded to fold-changes of >2 or <0.5 , respectively.

Bioinformatics. The function of proteins that exhibited a significant change in expression with CP treatment was investigated. These sequences were processed by examining their functional annotations in the Database for Annotation, Visualization, and Integrated Discovery (DAVID) version 6.8 (<http://david.abcc.ncifcrf.gov/home.jsp>) (39-41).

Western blot analysis. Total protein (5 μ g) that had been extracted from CP-treated cells was added to each well of an SDS-PAGE gel and electrophoresis was performed under reducing conditions. The separated proteins were transferred to polyvinylidene fluoride membranes (Merck KGaA) for 30 min at 15 V. After blocking in TBS-Tween-20 (0.1%) buffer with 5% skimmed milk for 2 h at room temperature, the membranes were incubated with an anti-calpain 1 antibody (1:1,000 dilution; cat. no. 2556; Cell Signaling Technology, Inc., Beverly, MA, USA) at 4°C overnight. The membranes were then washed and incubated with horseradish peroxidase-conjugated anti-rabbit immunoglobulin (Ig)G antibody (cat. no. A106PU; American Qualex, San Clemente, CA, USA) at room temperature for 1 h. The blots were washed and visualized with SuperSignal West Dura Extended Duration substrate (Thermo Fisher Scientific, Inc.). The bands were analyzed with the myECL Imager system (version 2.0; Thermo Fisher Scientific, Inc.). Next, the membranes were stripped by Restore Western Blot Stripping buffer (Thermo Fisher Scientific, Inc.), and the same membranes were re-probed with an anti- β -actin antibody (1:5,000 dilution; cat. no. sc-47778; Santa Cruz Biotechnology, Inc., Dallas, TX, USA) at 4°C overnight, which served as the protein loading control. The intensities of calpain-1 and β -actin were quantified with myImageAnalysis software (version 2.0; Thermo Fisher Scientific, Inc.). The relative quantities of calpain-1 over β -actin were used to evaluate calpain-1 expression under different conditions. All western blot analyses were performed as three independent experiments.

Reverse transcription-quantitative polymerase chain reaction (RT-qPCR). Total RNA was extracted from HaCaT cells with the GenElute Mammalian Total RNA Miniprep kit (cat. no. RTN70-1KT; Sigma-Aldrich; Merck KGaA). Complementary (c)DNA was synthesized with the High Capacity cDNA Reverse Transcription kit (cat. no. 4368814; Thermo Fisher Scientific, Inc.) according to the manufacturer's protocols. To measure the expression levels of interleukin (IL)-1 α , IL-6, IL-8 and tumor necrosis factor (TNF)- α , PCR amplification was performed in the 7500 system (Applied Biosystems; Thermo Fisher Scientific, Inc.). Primers and TaqMan probes for detecting IL-1 α (assay ID, Hs00174092_m1), IL-6 (assay ID, Hs00985639_m1), IL-8 (assay ID, Hs00174103_m1), TNF- α (assay ID, Hs01113624_g1) and 18S ribosomal (r)RNA (assay ID, Hs03928990_g1) were supplied with the TaqMan Gene Expression Assay (Applied

Biosystems; Thermo Fisher Scientific, Inc.). The relative gene expression was calculated via the $\Delta\Delta C_q$ method (42-46). The $\Delta\Delta C_q$ method uses the normalized ΔC_q value of each sample, which was calculated with 18S rRNA as the endogenous control gene. The $\Delta\Delta C_q$ value is the difference between treated and control samples. Finally, the fold-change was determined as $2^{-\Delta\Delta C_q}$. Gene expression was evaluated in triplicate.

Statistical analysis. All data are presented as the mean \pm standard error of the mean. The data were analyzed by one-way analysis of variance followed by Dunnett's test or the unpaired Student's t-test for two groups. $P < 0.05$ was considered to indicate a significant difference. Computations were performed with GraphPad Prism version 5.1 (GraphPad Software Inc., La Jolla, CA, USA).

Results

Tryptic digestion of collagen from soft-shelled turtle. Collagen extracted from soft-shelled turtle was digested with trypsin to obtain CPs with molecular weights of <3.5 kDa. The collagen digestion was monitored by extracting samples at different time-points. The samples were separated on a 15% tricine-SDS-PAGE gel (Fig. 1A). After 1 h of trypsin digestion, bands that corresponded to collagen or CPs at around 42 kDa were observed (Fig. 1A; black square). After 96 h, these bands completely disappeared (Fig. 1A). The molecular weight distribution of the digested CPs was evaluated using MALDI-TOF/MS. The results indicated that the collagen was digested to CPs with a molecular weight of <4.0 kDa, and most CPs had mass-to-charge (m/z) ratios of 800-2,500 (Fig. 1B).

Cytotoxicity of CPs to HaCaT cells. To examine the possible cytotoxic effects of CPs on HaCaT cells, it was assessed whether the cell growth rate was affected when the cells were grown in culture medium containing CPs at concentrations of 0.1-100 μ g/ml. The results indicated that CPs did not inhibit the HaCaT cell growth rate at any of the tested concentrations (Fig. 2). Therefore, the CPs were used at a concentration of 100 μ g/ml in the subsequent experiments.

Identification and semi-quantitative comparison of differentially expressed proteins in CP-treated HaCaT cells. Next, the potential effect of CPs on cells in the basal layer of the skin was investigated by treating HaCaT cells with CPs. To determine the molecular profile of proteins that are regulated by CPs, a shotgun proteomics approach was used. A label-free semi-quantitative method based on spectral counting was utilized to evaluate the proteins expressed in HaCaT cells. The Rsc values were calculated for proteins that had been identified in CP-treated HaCaT cells and untreated cells. A positive value indicated increased expression by CP-treatment and a negative value indicated reduced expression by CP-treatment (Fig. 3; light grey area). For each protein that had been identified in CP-treated HaCaT cells and untreated cells, the NSAF value was also calculated (Fig. 3; black bars; peptides, grey bar; control). Proteins with a >1 and <-1 Rsc value were considered candidate CP-regulated proteins.

Based on this semi-quantitative procedure, a total of 211 proteins that were differentially expressed with CP treatment were identified (Table I). The expression of housekeeping

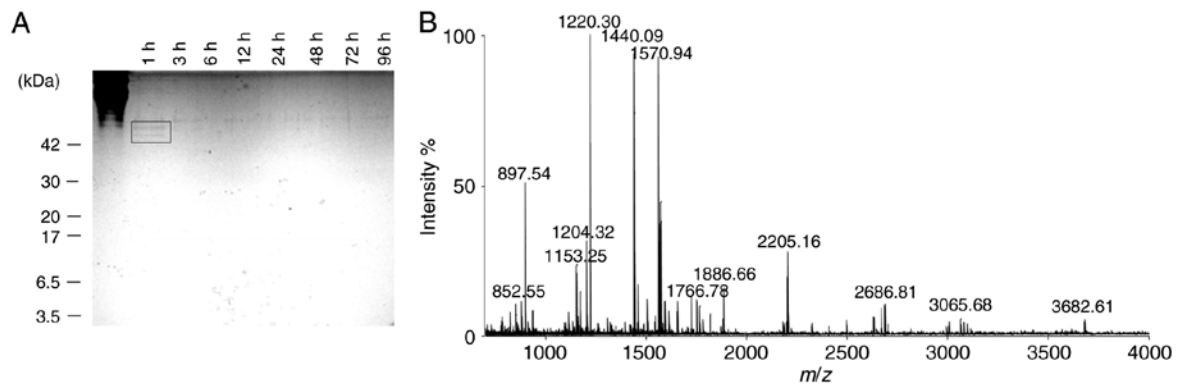


Figure 1. Characterization of collagen peptides obtained by digesting soft-shelled turtle collagen with trypsin. (A) Protein profiles of tryptic digestion products obtained using 15% tricine-SDS-PAGE. Samples were extracted at the indicated incubation times. Molecular weight markers (kDa) are indicated on the left. (B) Matrix-assisted laser desorption/ionization-time-of-flight/mass spectrometry positive ion mass spectra of digested collagen peptides mixture. The m/z values are stated above the corresponding peaks. m/z , mass to charge ratio.

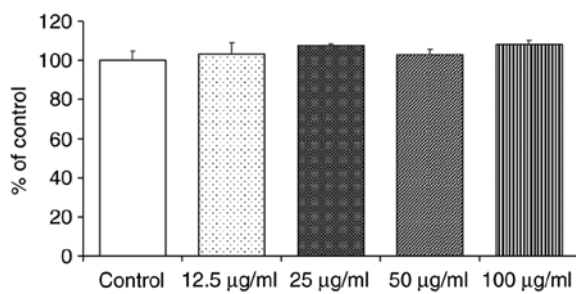


Figure 2. Cytotoxic effect of collagen peptides on HaCaT cells. Different concentrations of collagen peptides were added to HaCaT cells. None of these concentrations affected the cell proliferation at 72 h.

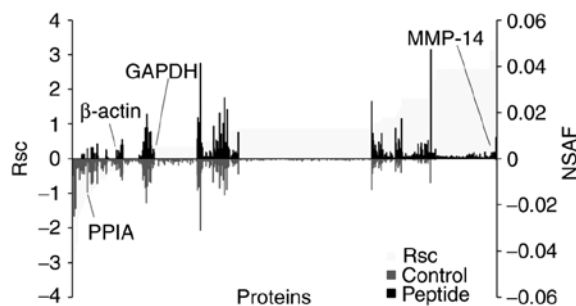


Figure 3. Semi-quantitative comparison of proteins in HaCaT cells that were differentially expressed with collagen peptide treatments. The Rsc and the NSAF values were calculated for identified proteins to compare protein expression levels between untreated (control) and collagen-peptide-treated HaCaT cells. Cell proteins are placed along the x-axis, ordered according to the Rsc value, increasing from left to right (light grey area). NSAF values from control cells are displayed below the axis (grey bars), and values from peptide-treated cells are placed above the axis (black bars). Proteins highly expressed in control and peptide-treated cells are near the left and right sides, respectively, of the x-axis. Housekeeping proteins are located near the center of the x-axis. Rsc, \log_2 of the ratio of protein abundance; NSAF, normalized spectral abundance factor; PPIA, peptidylprolyl isomerase A; MMP, matrix metalloproteinase.

proteins, including β -actin and GAPDH, was not altered by CP treatment.

Functional annotation of proteins regulated by CPs. A gene ontology (GO) analysis of the candidate CP-regulated proteins

was then performed. GO terms associated with 'pathway' (Fig. 4A) and 'molecular function' (Fig. 4B) were searched for in DAVID. The search focused on proteins classified as 'protein processing in endoplasmic reticulum' (Table II).

Effect of CP on calpain-1 expression in HaCaT cells. To confirm that CP treatment altered calpain-1 expression, calpain-1 protein levels were examined in CP-treated HaCaT cells. It was identified that calpain-1 expression was significantly increased with CP treatment compared with that in control cells (Fig. 5).

Effect of CP treatment on the expression of inflammatory factors in HaCaT cells. To investigate whether the CP-induced increase in calpain-1 expression was associated with the expression of inflammatory cytokines in HaCaT cells, expression levels of IL-1 α , IL-6, IL-8 and TNF- α were examined (Fig. 6). Although CP-treated HaCaT cells tended to exhibit increases in IL-1 α expression (Fig. 6A), the change was not significant ($P=0.0781$). However, IL-6 expression was significantly decreased in HaCaT cells treated with CP, and by contrast, IL-8 expression was significantly increased with CP treatment (Fig. 6B and C). Finally, CPs had no effect on TNF- α expression (Fig. 6D).

Discussion

In the present study, a gel-free LC-MS-based proteomics approach was used to examine the functional effects of soft-shelled turtle CPs on human skin cells. A total of 211 proteins that exhibited >2-fold changes in expression after CP treatment were successfully identified in HaCaT cells, based on a semi-quantitative method of spectral counting. To examine the roles of these identified proteins, a GO analysis was performed. The study focused on the functions of proteins classified as 'protein processing in endoplasmic reticulum', as they have important roles in the synthesis of correctly folded proteins and in the degradation of misfolded proteins. The function of calpain-1, which is a member of this pathway, was also examined.

To validate the spectral counting results, a western blot analysis was performed to examine whether calpain-1

Table I. Proteins differentially expressed (≥ 2 -fold) after treatment with collagen peptides.

ID	Accession number	Definition	Number of amino acids	Fold change (Rsc)
TBA1B_HUMAN	P68363	Tubulin α -1B chain	451	-2.937
H2B1L_HUMAN	Q99880	Histone H2B type 1-L	126	-2.890
H2B1B_HUMAN	P33778	Histone H2B type 1-B	126	-2.683
H2B1K_HUMAN	O60814	Histone H2B type 1-K	126	-2.683
K2C75_HUMAN	O95678	Keratin, type II cytoskeletal 75	551	-2.507
K2C4_HUMAN	P19013	Keratin, type II cytoskeletal 4	534	-2.443
K2C79_HUMAN	Q5XKE5	Keratin, type II cytoskeletal 79	535	-2.073
ATPA_HUMAN	P25705	ATP synthase subunit α , mitochondrial	553	-2.073
HS902_HUMAN	Q14568	Putative heat shock protein HSP 90- α A2	343	-1.691
HSP7C_HUMAN	P11142	Heat shock cognate 71 kDa protein	646	-1.577
H2A1B_HUMAN	P04908	Histone H2A type 1-B/E	130	-1.577
K2C6C_HUMAN	P48668	Keratin, type II cytoskeletal 6C	564	-1.409
K2C5_HUMAN	P13647	Keratin, type II cytoskeletal 5	590	-1.384
TBA3C_HUMAN	Q13748	Tubulin α -3C/D chain	450	-1.383
HS90B_HUMAN	P08238	Heat shock protein HSP 90- β	724	-1.343
K1C19_HUMAN	P08727	Keratin, type I cytoskeletal 19	400	-1.245
TBA3E_HUMAN	Q6PEY2	Tubulin α -3E chain	450	-1.171
TPIS_HUMAN	P60174	Triosephosphate isomerase	286	-1.171
LMNA_HUMAN	P02545	Prelamin-A/C	664	-1.171
K2C3_HUMAN	P12035	Keratin, type II cytoskeletal 3	628	-1.171
PPIA_HUMAN	P62937	Peptidyl-prolyl cis-trans isomerase A	165	-1.125
K2C73_HUMAN	Q86Y46	Keratin, type II cytoskeletal 73	540	-1.005
HS904_HUMAN	Q58FG1	Putative heat shock protein HSP 90- α A4	418	-1.005
RS12_HUMAN	P25398	40S ribosomal protein S12	132	-1.005
H2A1A_HUMAN	Q96QV6	Histone H2A type 1-A	131	-1.005
FAS_HUMAN	P49327	Fatty acid synthase	2,511	-1.005
K1C18_HUMAN	P05783	Keratin, type I cytoskeletal 18	430	1.009
KRT84_HUMAN	Q9NSB2	Keratin, type II cuticular Hb4	600	1.029
H2B1A_HUMAN	Q96A08	Histone H2B type 1-A	127	1.029
PSA2_HUMAN	P25787	Proteasome subunit α type-2	234	1.029
PHB2_HUMAN	Q99623	Prohibitin-2	299	1.029
ALBU_HUMAN	P02768	Serum albumin	609	1.029
SPTN1_HUMAN	Q13813	Spectrin α chain, non-erythrocytic 1	2,472	1.029
S10AE_HUMAN	Q9HCY8	Protein S100-A14	104	1.029
HSPB1_HUMAN	P04792	Heat shock protein β -1	205	1.029
PDIA3_HUMAN	P30101	Protein disulfide-isomerase A3	505	1.071
1433S_HUMAN	P31947	14-3-3 protein σ	248	1.071
ACTG_HUMAN	P63261	Actin, cytoplasmic 2	375	1.076
ACTBM_HUMAN	Q9BYX7	Putative β -actin-like protein 3	375	1.165
RSSA_HUMAN	P08865	40S ribosomal protein SA	295	1.165
IASPP_HUMAN	Q8WUF5	RelA-associated inhibitor	828	1.190
FUMH_HUMAN	P07954	Fumarate hydratase, mitochondrial	510	1.190
HMGB1_HUMAN	P09429	High mobility group protein B1	215	1.190
COR1B_HUMAN	Q9BR76	Coronin-1B	489	1.190
COTL1_HUMAN	Q14019	Coactosin-like protein	142	1.190
LA_HUMAN	P05455	Lupus La protein	408	1.190
NCBP1_HUMAN	Q09161	Nuclear cap-binding protein subunit 1	790	1.190
SQRD_HUMAN	Q9Y6N5	Sulfide:Quinone oxidoreductase, mitochondrial	450	1.190
TRAP1_HUMAN	Q12931	Heat shock protein 75 kDa, mitochondrial	704	1.190
EZRI_HUMAN	P15311	Ezrin	586	1.190
RL22_HUMAN	P35268	60S ribosomal protein L22	128	1.190

Table I. Continued.

ID	Accession number	Definition	Number of amino acids	Fold change (Rsc)
RS3_HUMAN	P23396	40S ribosomal protein S3	243	1.190
ARF4_HUMAN	P18085	ADP-ribosylation factor 4	180	1.190
COR1C_HUMAN	Q9ULV4	Coronin-1C	474	1.190
MARE1_HUMAN	Q15691	Microtubule-associated protein RP/EB family member 1	268	1.190
MYO1B_HUMAN	O43795	Unconventional myosin-Ib	1,136	1.190
FREM1_HUMAN	Q5H8C1	FRAS1-related extracellular matrix protein 1	2,179	1.190
VPS35_HUMAN	Q96QK1	Vacuolar protein sorting-associated protein 35	796	1.190
TBA1C_HUMAN	Q9BQE3	Tubulin α -1C chain	449	1.242
PRDX6_HUMAN	P30041	Peroxiredoxin-6	224	1.257
SERPH_HUMAN	P50454	Serpin H1	418	1.257
AN32B_HUMAN	Q92688	Acidic leucine-rich nuclear phosphoprotein 32 family member B	251	1.334
CX6B1_HUMAN	P14854	Cytochrome c oxidase subunit 6B1	86	1.334
ROA1_HUMAN	P09651	Heterogeneous nuclear ribonucleoprotein A1	372	1.334
COX5A_HUMAN	P20674	Cytochrome c oxidase subunit 5A, mitochondrial	150	1.417
PSME1_HUMAN	Q06323	Proteasome activator complex subunit 1	249	1.417
4F2_HUMAN	P08195	4F2 cell-surface antigen heavy chain	630	1.417
K1C9_HUMAN	P35527	Keratin, type I cytoskeletal 9	623	1.528
LEG7_HUMAN	P47929	Galectin-7	136	1.721
EIF3M_HUMAN	Q7L2H7	Eukaryotic translation initiation factor 3 subunit M	374	1.721
HNRDL_HUMAN	O14979	Heterogeneous nuclear ribonucleoprotein D-like	420	1.721
TCPB_HUMAN	P78371	T-complex protein 1 subunit β	535	1.721
CPNE3_HUMAN	O75131	Copine-3	537	1.721
DEST_HUMAN	P60981	Destrin	165	1.721
TFR1_HUMAN	P02786	Transferrin receptor protein 1	760	1.721
CNDP2_HUMAN	Q96KP4	Cytosolic non-specific dipeptidase	475	1.721
AHSA1_HUMAN	O95433	Activator of 90 kDa heat shock protein ATPase homolog 1	338	1.721
DDB1_HUMAN	Q16531	DNA damage-binding protein 1	1,140	1.721
ICAL_HUMAN	P20810	Calpastatin	708	1.721
ASNA_HUMAN	O43681	ATPase ASNA1	348	1.721
CISY_HUMAN	O75390	Citrate synthase, mitochondrial	466	1.721
CSK23_HUMAN	Q8NEV1	Casein kinase II subunit α 3	391	1.721
CNN2_HUMAN	Q99439	Calponin-2	309	1.721
SYYC_HUMAN	P54577	Tyrosine-tRNA ligase, cytoplasmic	528	1.721
SODM_HUMAN	P04179	Superoxide dismutase [Mn], mitochondrial	222	1.721
ACTY_HUMAN	P42025	B-centractin	376	1.721
ML12A_HUMAN	P19105	Myosin regulatory light chain 12A	171	1.721
RL32_HUMAN	P62910	60S ribosomal protein L32	135	1.721
MYO1C_HUMAN	O00159	Unconventional myosin-Ic	1,063	1.721
FSCN1_HUMAN	Q16658	Fascin	493	1.722
RL3_HUMAN	P39023	60S ribosomal protein L3	403	1.722
RPN1_HUMAN	P04843	Dolichyl-diphosphooligosaccharide-protein glycosyltransferase subunit 1	607	1.722
B2MG_HUMAN	P61769	B-2-microglobulin	119	1.722
RBP56_HUMAN	Q92804	TATA-binding protein-associated factor 2N	592	1.722
2AAA_HUMAN	P30153	Serine/threonine-protein phosphatase 2A 65 kDa regulatory subunit A α isoform	589	1.722
ENOG_HUMAN	P09104	Γ -enolase	434	1.722
RL27A_HUMAN	P46776	60S ribosomal protein L27a	148	1.722
DCD_HUMAN	P81605	Dermcidin	110	1.722

Table I. Continued.

ID	Accession number	Definition	Number of amino acids	Fold change (Rsc)
RS7_HUMAN	P62081	40S ribosomal protein S7	194	1.722
IQGA1_HUMAN	P46940	Ras GTPase-activating-like protein IQGAP1	1,657	1.723
TERA_HUMAN	P55072	Transitional endoplasmic reticulum ATPase	806	1.723
SPTB2_HUMAN	Q01082	Spectrin β chain, non-erythrocytic 1	2,364	1.723
RL18A_HUMAN	Q02543	60S ribosomal protein L18a	176	1.723
CALX_HUMAN	P27824	Calnexin	592	1.723
TBA4B_HUMAN	Q9H853	Putative tubulin-like protein α -4B	241	1.724
TCPE_HUMAN	P48643	T-complex protein 1 subunit ϵ	541	1.724
K2C80_HUMAN	Q6KB66	Keratin, type II cytoskeletal 80	452	1.724
HNRPK_HUMAN	P61978	Heterogeneous nuclear ribonucleoprotein K	463	1.865
VPP4_HUMAN	Q9HBG4	V-type proton ATPase 116 kDa subunit a isoform 4	840	2.029
EF1G_HUMAN	P26641	Elongation factor 1- γ	437	2.110
G6PI_HUMAN	P06744	Glucose-6-phosphate isomerase	558	2.110
H2B1M_HUMAN	Q99879	Histone H2B type 1-M	126	2.119
RALY_HUMAN	Q9UKM9	RNA-binding protein Raly	306	2.253
TXTP_HUMAN	P53007	Tricarboxylate transport protein, mitochondrial	311	2.253
CAN1_HUMAN	P07384	Calpain-1 catalytic subunit	714	2.253
DHB12_HUMAN	Q53GQ0	Estradiol 17- β -dehydrogenase 12	312	2.253
DHX9_HUMAN	Q08211	ATP-dependent RNA helicase A	1,270	2.253
MYADM_HUMAN	Q96S97	Myeloid-associated differentiation marker	322	2.253
CUTA_HUMAN	O60888	Protein CutA	179	2.253
CECR2_HUMAN	Q9BXF3	Cat eye syndrome critical region protein 2	1,484	2.253
KRT81_HUMAN	Q14533	Keratin, type II cuticular Hb1	505	2.569
GLOD4_HUMAN	Q9HC38	Glyoxalase domain-containing protein 4	313	2.569
SURF4_HUMAN	O15260	Surfeit locus protein 4	269	2.569
P4HA1_HUMAN	P13674	Prolyl 4-hydroxylase subunit α -1	534	2.569
ANX11_HUMAN	P50995	Annexin A11	505	2.569
CALU_HUMAN	O43852	Calumenin	315	2.569
TFG_HUMAN	Q92734	Protein TFG	400	2.569
ECHA_HUMAN	P40939	Trifunctional enzyme subunit α , mitochondrial	763	2.569
PA2G4_HUMAN	Q9UQ80	Proliferation-associated protein 2G4	394	2.569
SF3A2_HUMAN	Q15428	Splicing factor 3A subunit 2	464	2.569
SHLB2_HUMAN	Q9NR46	Endophilin-B2	395	2.569
MBOA7_HUMAN	Q96N66	Lysophospholipid acyltransferase 7	472	2.569
AT1A1_HUMAN	P05023	Sodium/potassium-transporting ATPase subunit α -1	1,023	2.569
PPME1_HUMAN	Q9Y570	Protein phosphatase methylesterase 1	386	2.569
IF4G2_HUMAN	P78344	Eukaryotic translation initiation factor 4 γ 2	907	2.569
IPYR2_HUMAN	Q9H2U2	Inorganic pyrophosphatase 2, mitochondrial	334	2.569
CKAP4_HUMAN	Q07065	Cytoskeleton-associated protein 4	602	2.569
COPB2_HUMAN	P35606	Coatomer subunit β	906	2.569
DLG1_HUMAN	Q12959	Disks large homolog 1	904	2.569
ATX2L_HUMAN	Q8WWM7	Ataxin-2-like protein	1,075	2.569
RMXL1_HUMAN	Q96E39	RNA binding motif protein, X-linked-like-1	390	2.569
CERS2_HUMAN	Q96G23	Ceramide synthase 2	380	2.569
RM46_HUMAN	Q9H2W6	39S ribosomal protein L46, mitochondrial	279	2.569
FDFT_HUMAN	P37268	Squalene synthase	417	2.569
CP26A_HUMAN	O43174	Cytochrome P450 26A1	497	2.569
EIF3A_HUMAN	Q14152	Eukaryotic translation initiation factor 3 subunit A	1,382	2.569
GLYM_HUMAN	P34897	Serine hydroxymethyltransferase, mitochondrial	504	2.569
ARHGJ_HUMAN	Q8IW93	Rho guanine nucleotide exchange factor 19	802	2.569

Table I. Continued.

ID	Accession number	Definition	Number of amino acids	Fold change (Rsc)
GFPT1_HUMAN	Q06210	Glutamine-fructose-6-phosphate aminotransferase [isomerizing] 1	699	2.569
NOD2_HUMAN	Q9HC29	Nucleotide-binding oligomerization domain-containing protein 2	1,040	2.569
NAGK_HUMAN	Q9UJ70	N-acetyl-D-glucosamine kinase	344	2.569
SYAC_HUMAN	P49588	Alanine-tRNA ligase, cytoplasmic	968	2.569
CLAP1_HUMAN	Q7Z460	CLIP-associating protein 1	1,538	2.569
SPTN4_HUMAN	Q9H254	Spectrin β chain, non-erythrocytic 4	2,564	2.569
MTU1_HUMAN	O75648	Mitochondrial tRNA-specific 2-thiouridylase 1	421	2.569
PAOX_HUMAN	Q6QHF9	Peroxisomal N(1)-acetyl-spermine/spermidine oxidase	649	2.569
MCM5_HUMAN	P33992	DNA replication licensing factor MCM5	734	2.569
WNK3_HUMAN	Q9BYP7	Serine/threonine-protein kinase WNK3	1,800	2.569
LIMK2_HUMAN	P53671	LIM domain kinase 2	638	2.569
VIPR2_HUMAN	P41587	Vasoactive intestinal polypeptide receptor 2	438	2.569
DOS_HUMAN	Q8N350	Protein Dos	725	2.569
TRDN_HUMAN	Q13061	Triadin O	729	2.569
ZN318_HUMAN	Q5VUA4	Zinc finger protein 318	2,279	2.569
SUCO_HUMAN	Q9UBS9	SUN domain-containing ossification factor	1,254	2.569
2AAB_HUMAN	P30154	Serine/threonine-protein phosphatase 2A 65 kDa regulatory subunit A β isoform	601	2.569
PCBP2_HUMAN	Q15366	Poly(rC)-binding protein 2	365	2.569
1433Z_HUMAN	P63104	14-3-3 protein ζ/δ	245	2.569
MDHC_HUMAN	P40925	Malate dehydrogenase, cytoplasmic	334	2.569
DNM1L_HUMAN	O00429	Dynamin-1-like protein	736	2.569
ARL8A_HUMAN	Q96BM9	ADP-ribosylation factor-like protein 8A	186	2.569
DIAP1_HUMAN	O60610	Protein diaphanous homolog 1	1,272	2.569
IF4H_HUMAN	Q15056	Eukaryotic translation initiation factor 4H	248	2.569
TEX35_HUMAN	Q5T0J7	Testis-expressed sequence 35 protein	233	2.569
GGCT_HUMAN	O75223	Γ -glutamylcyclotransferase	188	2.569
SF3A1_HUMAN	Q15459	Splicing factor 3A subunit 1	793	2.569
ARPC2_HUMAN	O15144	Actin-related protein 2/3 complex subunit 2	300	2.569
PP14B_HUMAN	Q96C90	Protein phosphatase 1 regulatory subunit 14B	147	2.569
ARHGH_HUMAN	Q96PE2	Rho guanine nucleotide exchange factor 17	2,063	2.569
SYSC_HUMAN	P49591	Serine-tRNA ligase, cytoplasmic	514	2.569
ALPK2_HUMAN	Q86TB3	A-protein kinase 2	2,170	2.569
SUSD3_HUMAN	Q96L08	Sushi domain-containing protein 3	255	2.569
DP13B_HUMAN	Q8NEU8	DCC-interacting protein 13- β	664	2.569
XRCC6_HUMAN	P12956	X-ray repair cross-complementing protein 6	609	2.569
HBS1L_HUMAN	Q9Y450	HBS1-like protein	684	2.569
RK_HUMAN	Q15835	Rhodopsin kinase	563	2.569
SPRY7_HUMAN	Q5W111	SPRY domain-containing protein 7	196	2.569
BRSK2_HUMAN	Q8IWQ3	Serine/threonine-protein kinase BRSK2	736	2.569
STAT1_HUMAN	P42224	Signal transducer and activator of transcription 1- α/β	750	2.569
ZEP1_HUMAN	P15822	Zinc finger protein 40	2,718	2.569
SOX4_HUMAN	Q06945	Transcription factor SOX-4	474	2.569
REXO1_HUMAN	Q8N1G1	RNA exonuclease 1 homolog	1,221	2.569
ZN521_HUMAN	Q96K83	Zinc finger protein 521	1,311	2.569
DLG5_HUMAN	Q8TDM6	Disks large homolog 5	1,919	2.569
TM155_HUMAN	Q4W5P6	Protein TMEM155	130	2.569
ZYX_HUMAN	Q15942	Zyxin	572	2.569

Table I. Continued.

ID	Accession number	Definition	Number of amino acids	Fold change (Rsc)
UBAC2_HUMAN	Q8NBM4	Ubiquitin-associated domain-containing protein 2	344	2.569
STPG2_HUMAN	Q8N412	Sperm-tail PG-rich repeat-containing protein 2	459	2.569
K0556_HUMAN	O60303	Uncharacterized protein KIAA0556	1,618	2.569
KLH11_HUMAN	Q9NVR0	Kelch-like protein 11	708	2.569
TTLL6_HUMAN	Q8N841	Tubulin polyglutamylase TTLL6	843	2.569
CFA36_HUMAN	Q96G28	Cilia- and flagella-associated protein 36	342	2.569
MMP14_HUMAN	P50281	Matrix metalloproteinase-14	582	3.101
ADT1_HUMAN	P12235	ADP/ATP translocase 1	298	3.101
GNPMB_HUMAN	Q14956	Transmembrane glycoprotein NMB	572	3.101
PYGL_HUMAN	P06737	Glycogen phosphorylase, liver form	847	3.101
NIPS2_HUMAN	O75323	Protein NipSnap homolog 2	286	3.101
ERP29_HUMAN	P30040	Endoplasmic reticulum resident protein 29	261	3.101
ADT3_HUMAN	P12236	ADP/ATP translocase 3	298	3.101
LBN_HUMAN	Q86UK5	Limbin	1,308	3.101
RAB1B_HUMAN	Q9H0U4	Ras-related protein Rab-1B	201	3.201
TF_HUMAN	P13726	Tissue factor	295	3.490

Rsc, log₂ of the ratio of protein abundance; ATP, adenosine triphosphate; ADP, adenosine diphosphate; FRAS-1, fraser syndrome 1; MCM, mini-chromosome maintenance; WNK, with no K (lysine); DCC, deleted in colorectal cancer.

Table II. Differentially expressed proteins categorized as 'protein processing in endoplasmic reticulum' in a Gene Ontology analysis in human skin keratinocytes.

Accession number	Description	Fold change (Rsc)
P11142	Heat shock cognate 71 kDa protein	-1.577
P08238	Heat shock protein HSP 90-β	-1.343
P30101	Protein disulfide-isomerase A3	1.071
P04843	Dolichyl-diphosphooligosaccharide-protein glycosyltransferase subunit 1	1.722
P27824	Calnexin	1.723
P55072	Transitional endoplasmic reticulum ATPase	1.723
P07384	Calpain-1 catalytic subunit	2.253
Q07065	Cytoskeleton-associated protein 4	2.569
P30040	Endoplasmic reticulum resident protein 29	3.101

Rsc, log₂ of the ratio of protein abundance.

expression is increased in HaCaT cells with CP treatment. Calpain-1 is a calcium-dependent intracellular cysteine protease (47,48). It has an important role in various biological processes, including cell proliferation, cell migration, apoptosis and cytoskeletal remodeling (49,50). Therefore, calpain is considered a therapeutic target for disorders involving inflammation, wound healing and tumor progression. A previous study reported that downregulation of calpain-1 expression in IgE-activated mast cells led to a reduced expression of cytokines, including IL-6 and TNF-α. Thus, they concluded that calpain-1 may regulate IgE-mediated allergic inflammation (51). Another study indicated that downregulation of calpain-1 expression in lung fibroblast cells also reduced the

expression of cytokines, including IL-6, IL-8, and TNF-α (52). Furthermore, calpain-1 knockout mice exhibited impaired bactericidal activity in an acute bacterial peritonitis model, due to a reduction in IL-1α production (53). Therefore, calpain-1 is considered a key factor in the immune response through its regulation of inflammation. Accordingly, it was hypothesized that CP-induced increases in calpain-1 expression in HaCaT cells may affect the expression of inflammatory cytokines in keratinocytes. The present results support this hypothesis. Therefore, CP treatment may regulate the immune system in the setting of skin wounds.

In the present GO analysis in the category molecular function, several proteins classified as 'cadherin binding

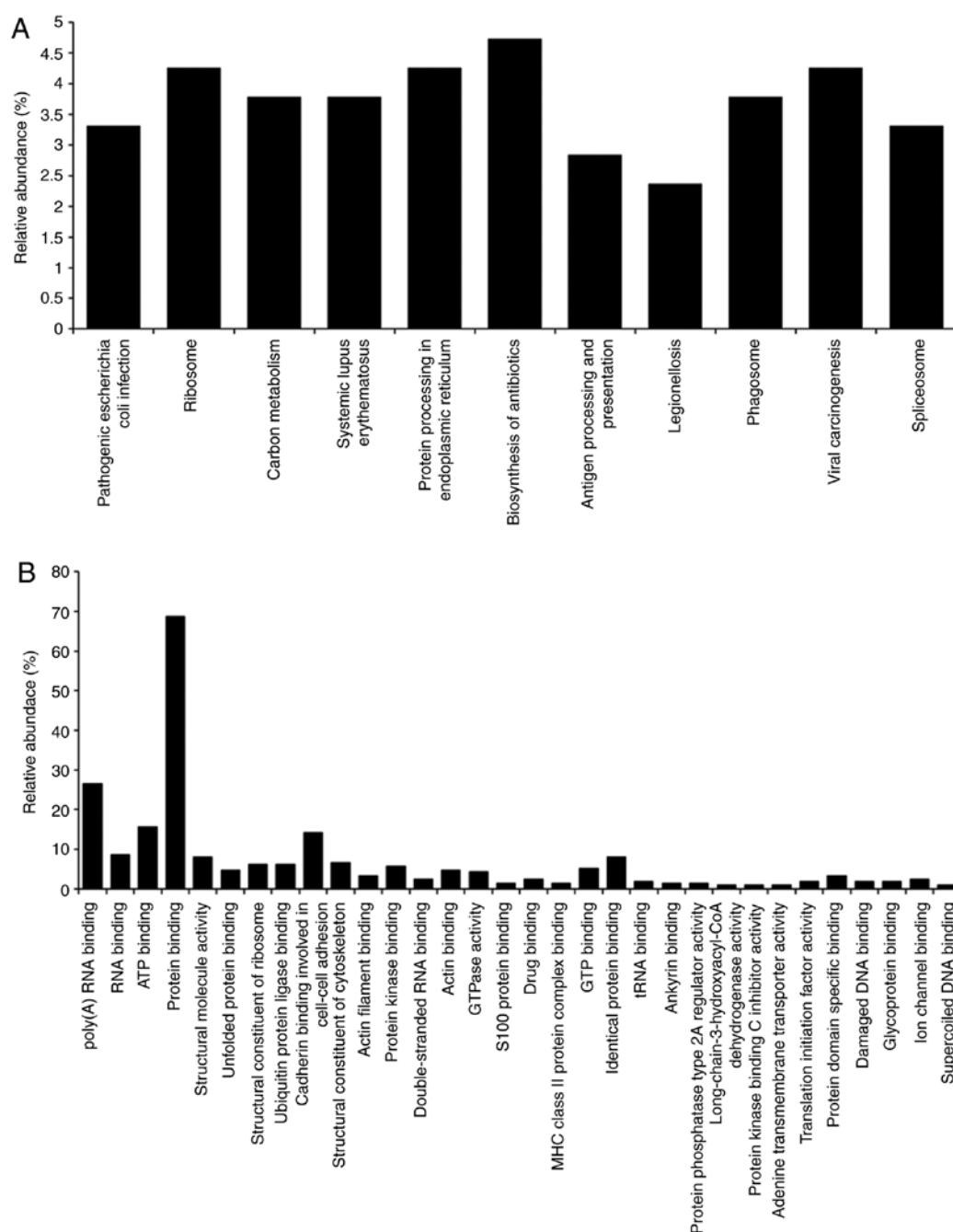


Figure 4. GO analysis of identified proteins. Differentially expressed proteins were assigned to KEGG signaling pathway and GO term categories. (A) KEGG signaling pathway terms. (B) GO molecular function terms. Only significant ($P < 0.05$) categories are shown. KEGG, Kyoto Encyclopedia of Genes and Genomes; GO, Gene Ontology; MHC, major histocompatibility complex.

involved in cell-cell adhesion' exhibited altered expression with CP treatment. A previous study by our group reported that in HaCaT cells, these proteins were changed by treatment with collagen derived from soft-shelled turtle. Furthermore, it was observed that changing the expression of these proteins enhanced the wound healing properties of HaCaT cells by inducing EMT (34). In the present study, it was revealed that CP treatment was associated with >2-fold increases in ceramide synthase 2 expression in HaCaT cells compared with that in control cells (Table I). Ceramide is an epidermal sphingolipid that has important roles in maintaining the skin barrier and supporting wound healing processes (54-56). The present result is similar to previous ones reported for collagen

derived from soft-shelled turtles and for CPs derived from other origins (25,31,32,57). It is therefore suggested that CPs from soft-shelled turtles may facilitate wound healing.

Although the present study suggested that CPs from soft-shelled turtles may be a useful material for pharmaceuticals and medical products, it remains elusive whether these CPs affect the wound healing processes in keratinocytes *in vivo*. Of note, certain CP-regulated inflammatory cytokines including IL-6 and IL-8 were not been investigated to determine their potential effects on the wound healing process in keratinocytes. Further *in vitro* and *in vivo* studies are necessary to clarify the effect of CPs from soft-shelled turtle on wound healing and the role of CP-regulated inflammatory

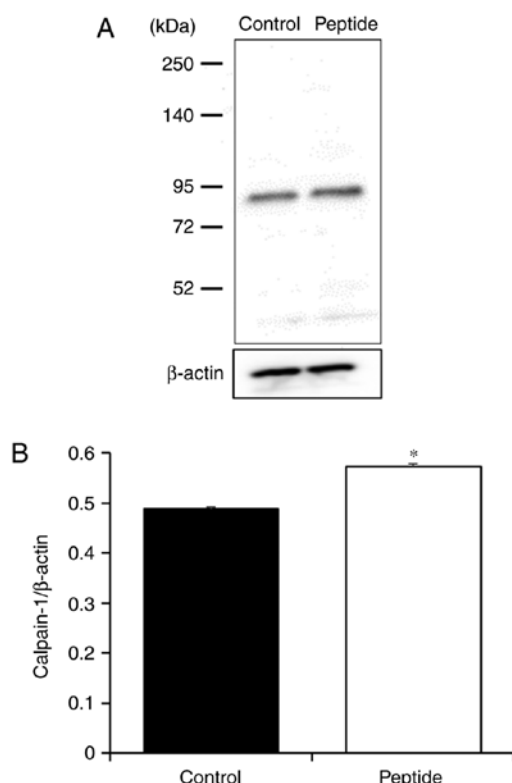


Figure 5. Expression of calpain-1 in collagen-peptide-treated HaCaT cells. (A) Western blot analysis indicates the expression levels of calpain-1 protein in HaCaT cells treated without (control) or with collagen peptides. (B) Quantification of western blot results. *P<0.05 vs. control.

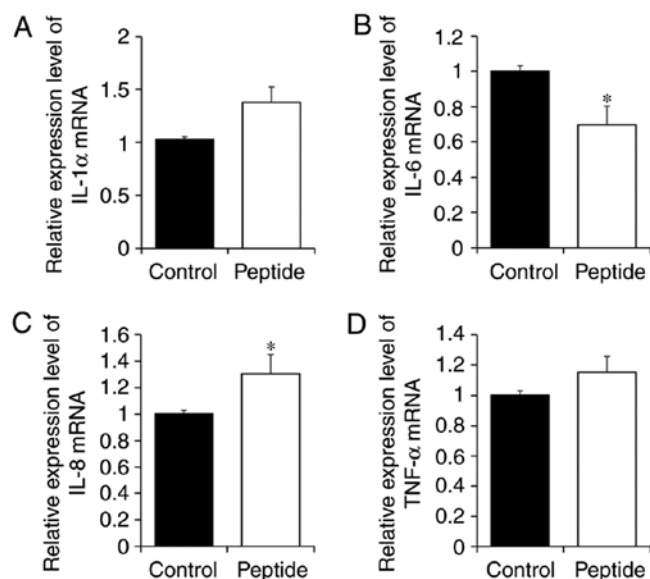


Figure 6. Cytokine expression changes in collagen-peptide treated HaCaT cells. Untreated cells (control) and collagen-peptide-treated HaCaT cells were analyzed by reverse-transcription quantitative polymerase chain reaction analysis. The collagen peptide-induced fold changes in the relative expression of inflammatory factors (A) IL-1α, (B) IL-6, (C) IL-8 and (D) TNF-α are indicated. The expression levels in the control group were set to 1, and the fold changes after collagen peptide treatment were evaluated using the $2^{-\Delta\Delta C_q}$ method. *P<0.05 vs. control. IL, interleukin; TNF, tumor necrosis factor.

cytokines in keratinocytes. In addition, it is also necessary to investigate the correlation between the expression of

calpain-1 and inflammatory cytokines in CP-treated keratinocytes.

In conclusion, the present shotgun LC/MS-based global proteomic analysis revealed that CP treatment regulated the expression of inflammatory cytokines in HaCaT cells and induced the expression of proteins associated with cell-cell adhesion and skin barrier maintenance. Therefore, CPs from soft-shelled turtles may provide significant benefits in maintaining the biological environment of the skin. These peptides may be a useful material for pharmaceuticals and medical products.

Acknowledgements

The authors are grateful to Mr. Takashi Aboshi (Shin-uoei, Inc.) for providing the soft-shelled turtle tissue used in the present study.

Funding

This study was supported in part by a Grant-in-Aid for Scientific Research (C) from the Japanese Society for the Promotion of Science to T.Y. (grant no. 15K09054).

Availability of data and materials

All data generated or analyzed during this study are included in this published article.

Authors' contributions

TY and AT designed the study and analyzed the data. TY and SN performed the experimental work. TY drafted the manuscript. KM contributed conduct the literature review. AT critically evaluated the study and final version of the manuscript. All authors participated in discussion of the study and gave final approval.

Ethical approval and consent to participate

Not applicable.

Consent for publication

Not applicable.

Competing interests

The authors declare that they have no competing interests.

References

- Gelse K, Pöschl E and Aigner T: Collagens-structure, function, and biosynthesis. *Adv Drug Deliv Rev* 55: 1531-1546, 2003.
- Myllyharju J and Kivirikko KI: Collagens, modifying enzymes and their mutations in humans, flies and worms. *Trends Genet* 20: 33-43, 2004.
- Birk DE and Trelstad RL: Extracellular compartments in tendon morphogenesis: Collagen fibril, bundle, and macroaggregate formation. *J Cell Biol* 103: 231-240, 1986.
- Adachi E and Hayashi T: Anchoring of epithelia to underlying connective tissue: Evidence of frayed ends of collagen fibrils directly merging with meshwork of lamina densa. *J Electron Microsc* (Tokyo) 43: 264-271, 1994.

5. Park KH and Bae YH: Phenotype of hepatocyte spheroids in Arg-GLY-Asp (RGD) containing a thermo-reversible extracellular matrix. *Biosci Biotechnol Biochem* 66: 1473-1478, 2002.
6. Liu B, Weinzimer SA, Gibson TB, Mascarenhas D and Cohen P: Type Ialpha collagen is an IGFBP-3 binding protein. *Growth Hormone IGF Res* 13: 89-97, 2003.
7. Di Lullo GA, Sweeney SM, Korkko J, Ala-Kokko L and San Antonio JD: Mapping the ligand-binding sites and disease-associated mutations on the most abundant protein in the human, type I collagen. *J Biol Chem* 277: 4223-4231, 2002.
8. Saby C, Buache E, Brassart-Pasco S, El Btaouri H, Courageot MP, Van Gulick L, Garnotel R, Jeannesson P and Morjani H: Type I collagen aging impairs discoidin domain receptor 2-mediated tumor cell growth suppression. *Oncotarget* 7: 24908-24927, 2016.
9. Maquoi E, Assent D, Detilleux J, Pequeux C, Foidart JM and Noël A: MT1-MMP protects breast carcinoma cells against type I collagen-induced apoptosis. *Oncogene* 31: 480-493, 2012.
10. Muralidharan N, Jeya Shakila R, Sukumar D and Jeyasekaran G: Skin, bone and muscle collagen extraction from the trash fish, leather jacket (*Odonus niger*) and their characterization. *J Food Sci Technol* 50: 1106-1113, 2013.
11. Wang Y and Regenstein JM: Effect of EDTA, HCl, and citric acid on Ca salt removal from Asian (silver) carp scales prior to gelatin extraction. *J Food Sci* 74: C426-C431, 2009.
12. Wang C, Zhan CL, Cai QF, Du CH, Liu GM, Su WJ and Cao MJ: Expression and characterization of common carp (*Cyprinus carpio*) matrix metalloproteinase-2 and its activity against type I collagen. *J Biotechnol* 177: 45-52, 2014.
13. Benjakul S, Thiansilakul Y, Visessanguan W, Roytrakul S, Kishimura H, Prodpran T and Meesane J: Extraction and characterisation of pepsin-solubilised collagens from the skin of bigeye snapper (*Priacanthus tayenus* and *Priacanthus macracanthus*). *J Sci Food Agric* 90: 132-138, 2010.
14. Nalinanon S, Benjakul S and Kishimura H: Collagens from the skin of arabesque greenling (*Pleurogrammus azonus*) solubilized with the aid of acetic acid and pepsin from albacore tuna (*Thunnus alalunga*) stomach. *J Sci Food Agric* 90: 1492-1500, 2010.
15. Tziveleka LA, Ioannou E, Tsiourvas D, Berillis P, Foufa E and Roussis V: Collagen from the marine sponges *Axinella cannabina* and *Suberites carnosus*: Isolation and morphological, biochemical, and biophysical characterization. *Mar Drugs* 15: E152, 2017.
16. Pallela R, Venkatesan J, Janapala VR and Kim SK: Biophysicochemical evaluation of chitosan-hydroxyapatite-marine sponge collagen composite for bone tissue engineering. *J Biomed Mater Res A* 100: 486-495, 2012.
17. Coelho RCG, Marques ALP, Oliveira SM, Diogo GS, Pirraco RP, Moreira-Silva J, Xavier JC, Reis RL, Silva TH and Mano JF: Extraction and characterization of collagen from Antarctic and Sub-Antarctic squid and its potential application in hybrid scaffolds for tissue engineering. *Mater Sci Eng C Mater Biol Appl* 78: 787-795, 2017.
18. Gorell ES, Leung TH, Khoo P and Lane AT: Purified type I collagen wound matrix improves chronic wound healing in patients with recessive dystrophic epidermolysis bullosa. *Pediatr Dermatol* 32: 220-225, 2015.
19. Shevchenko RV, Sibbons PD, Sharpe JR and James SE: Use of a novel porcine collagen paste as a dermal substitute in full-thickness wounds. *Wound Repair Regen* 16: 198-207, 2008.
20. Wollina U, Meseg A and Weber A: Use of a collagen-elastin matrix for hard to treat soft tissue defects. *Int Wound J* 8: 291-296, 2011.
21. Barhoumi A, Salvador-Culla B and Kohane DS: NIR-triggered drug delivery by collagen-mediated second harmonic generation. *Adv Healthc Mater* 4: 1159-1163, 2015.
22. Wallace DG and Rosenblatt J: Collagen gel systems for sustained delivery and tissue engineering. *Adv Drug Deliv Rev* 55: 1631-1649, 2003.
23. Friess W: Collagen-biomaterial for drug delivery. *Eur J Pharm Biopharm* 45: 113-136, 1998.
24. Song H, Zhang S, Zhang L and Li B: Effect of orally administered collagen peptides from bovine bone on skin aging in chronologically aged mice. *Nutrients* 9: E1209, 2017.
25. Hu Z, Yang P, Zhou C, Li S and Hong P: Marine collagen peptides from the skin of Nile Tilapia (*Oreochromis niloticus*): Characterization and wound healing evaluation. *Mar Drugs* 15: E102, 2017.
26. Zhuang Y, Hou H, Zhao X, Zhang Z and Li B: Effects of collagen and collagen hydrolysate from jellyfish (*Rhopilema esculentum*) on mice skin photoaging induced by UV irradiation. *J Food Sci* 74: H183-H188, 2009.
27. Zague V: A new view concerning the effects of collagen hydrolysate intake on skin properties. *Arch Dermatol Res* 300: 479-483, 2008.
28. Fan J, Zhuang Y and Li B: Effects of collagen and collagen hydrolysate from jellyfish umbrella on histological and immunity changes of mice photoaging. *Nutrients* 5: 223-233, 2013.
29. Hou H, Li B, Zhang Z, Xue C, Yu G, Wang J, Bao Y, Bu L, Sun J, Peng Z and Su S: Moisture absorption and retention properties, and activity in alleviating skin photodamage of collagen polypeptide from marine fish skin. *Food Chem* 135: 1432-1439, 2012.
30. Song H, Meng M, Cheng X, Li B and Wang C: The effect of collagen hydrolysates from silver carp (*Hypophthalmichthys molitrix*) skin on UV-induced photoaging in mice: Molecular weight affects skin repair. *Food Funct* 8: 1538-1546, 2017.
31. Zhang Z, Wang J, Ding Y, Dai X and Li Y: Oral administration of marine collagen peptides from Chum Salmon skin enhances cutaneous wound healing and angiogenesis in rats. *J Sci Food Agric* 91: 2173-2179, 2011.
32. Wang J, Xu M, Liang R, Zhao M, Zhang Z and Li Y: Oral administration of marine collagen peptides prepared from chum salmon (*Oncorhynchus keta*) improves wound healing following cesarean section in rats. *Food Nutr Res* 59: 26411, 2015.
33. Yamamoto T, Uemura K, Sawashi Y, Mitamura K and Taga A: Optimization of method to extract collagen from 'Emperor' tissue of soft-shelled turtles. *J Oleo Sci* 65: 169-175, 2016.
34. Yamamoto T, Nakanishi S, Mitamura K and Taga A: Shotgun label-free proteomic analysis for identification of proteins in HaCaT human skin keratinocytes regulated by the administration of collagen from soft-shelled turtle. *J Biomed Mater Res B Appl Biomater*, 2017.
35. Schägger H: Tricine-SDS-PAGE. *Nat Protoc* 1: 16-22, 2006.
36. Bluemlein K and Ralser M: Monitoring protein expression in whole-cell extracts by targeted label- and standard-free LC-MS/MS. *Nat Protoc* 6: 859-869, 2011.
37. Old WM, Meyer-Arendt K, Aveline-Wolf L, Pierce KG, Mendoza A, Sevinsky JR, Resing KA and Ahn NG: Comparison of label-free methods for quantifying human proteins by shotgun proteomics. *Mol Cell Proteomics* 4: 1487-1502, 2005.
38. Zybilov B, Coleman MK, Florens L and Washburn MP: Correlation of relative abundance ratios derived from peptide ion chromatograms and spectrum counting for quantitative proteomic analysis using stable isotope labeling. *Anal Chem* 77: 6218-6224, 2005.
39. Dennis G Jr, Sherman BT, Hosack DA, Yang J, Gao W, Lane HC and Lempicki RA: DAVID: Database for annotation, visualization, and integrated discovery. *Genome Biol* 4: P3, 2003.
40. Huang da W, Sherman BT and Lempicki RA: Systematic and integrative analysis of large gene lists using DAVID bioinformatics resources. *Nat Protoc* 4: 44-57, 2009.
41. Huang da W, Sherman BT and Lempicki RA: Bioinformatics enrichment tools: Paths toward the comprehensive functional analysis of large gene lists. *Nucleic Acids Res* 37: 1-13, 2009.
42. Parikh P, Bai H, Swartz MF, Alfieri GM and Dean DA: Identification of differentially regulated genes in human patent ductus arteriosus. *Exp Biol Med* (Maywood) 241: 2112-2118, 2016.
43. Livak KJ and Schmittgen TD: Analysis of relative gene expression data using real-time quantitative PCR and the 2(-Delta Delta C(T)) method. *Methods* 25: 402-408, 2001.
44. Carbotti G, Nikpoor AR, Vacca P, Gangemi R, Giordano C, Campelli F, Ferrini S and Fabbì M: IL-27 mediates HLA class I up-regulation, which can be inhibited by the IL-6 pathway, in HLA-deficient small cell lung cancer cells. *J Exp Clin Cancer Res* 36: 140, 2017.
45. Adnan M, Morton G and Hadi S: Analysis of rpoS and bolA gene expression under various stress-induced environments in planktonic and biofilm phase using 2(-Delta Delta C(T)) method. *Mol Cell Biochem* 357: 275-282, 2011.
46. Soejima M and Koda Y: TaqMan-based real-time polymerase chain reaction for detection of FUT2 copy number variations: Identification of novel Alu-mediated deletion. *Transfusion* 51: 762-769, 2011.
47. Goll DE, Thompson VF, Li H, Wei W and Cong J: The calpain system. *Physiol Rev* 83: 731-801, 2003.
48. Momeni HR: Role of calpain in apoptosis. *Cell J* 13: 65-72, 2011.
49. Glading A, Lauffenburger DA and Wells A: Cutting to the chase: Calpain proteases in cell motility. *Trends Cell Biol* 12: 46-54, 2002.
50. Sorimachi H, Ishiura S and Suzuki K: Structure and physiological function of calpains. *Biochem J* 328: 721-732, 1997.

51. Wu Z, Chen X, Liu F, Chen W, Wu P, Wieschhaus AJ, Chishti AH, Roche PA, Chen WM and Lin TJ: Calpain-1 contributes to IgE-mediated mast cell activation. *J Immunol* 192: 5130-5139, 2014.
52. Yin G, Zeng Q, Zhao H, Wu P, Cai S, Deng L and Jiang W: Effect and mechanism of calpains on pediatric lobar pneumonia. *Bioengineered* 8: 374-382, 2017.
53. Kumar V, Everingham S, Hall C, Greer PA and Craig AW: Calpains promote neutrophil recruitment and bacterial clearance in an acute bacterial peritonitis model. *Eur J Immunol* 44: 831-841, 2014.
54. Kim H, Kim J, Park J, Kim SH, Uchida Y, Holleran WM and Cho Y: Water extract of gromwell (*Lithospermum erythrorhizon*) enhances migration of human keratinocytes and dermal fibroblasts with increased lipid synthesis in an in vitro wound scratch model. *Skin Pharmacol Physiol* 25: 57-64, 2012.
55. Amen N, Mathow D, Rabionet M, Sandhoff R, Langbein L, Gretz N, Jäckel C, Gröne HJ and Jennemann R: Differentiation of epidermal keratinocytes is dependent on glucosylceramide: Ceramide processing. *Hum Mol Genet* 22: 4164-4179, 2013.
56. Meckfessel MH and Brandt S: The structure, function, and importance of ceramides in skin and their use as therapeutic agents in skin-care products. *J Am Acad Dermatol* 71: 177-184, 2014.
57. Gangwar M, Gautam MK, Ghildiyal S, Nath G and Goel RK: *Mallotus philippinensis* Muell. Arg fruit glandular hairs extract promotes wound healing on different wound model in rats. *BMC Complement Altern Med* 15: 123, 2015.